the American Control Conference, Vol. 3, Pergemon, New York, 1995, pp. 1995–1999.
[13]Blakelock, J. H., *Automatic Control of Aircraft and Missiles*, 2nd ed., Wiley, New York, 1991.

Adaptive Output Feedback Control Methodology: Theory and Practical Implementation Aspects

Moshe Idan*
Technion—Israel Institute of Technology, 32000 Haifa, Israel
Anthony J. Calise†
Georgia Institute of Technology, Atlanta, Georgia 30332
and
Naira Hovakimyan‡
Virginia Polytechnic Institute and State University, Blacksburg, Virginia 24061

Introduction

ADAPTIVE output feedback control using universal function approximators, such as artificial neural networks (NNs), is motivated by the multitude of practical applications for which accurate modeling is challenging or may even be impossible.[1–3] Recently, two direct output feedback approaches that do not rely on state estimation were presented in Refs. 4 and 5. These approaches incorporate similar approximate output feedback linearization, linear dynamic compensation of the ideally linearized model, and different adaptive NN-based elements to compensate for the model linearization errors. The design of the linear compensator may be challenging for systems with high relative degree r, requiring stabilization of r poles at the origin resulting from standard linearization.

The current work examines an extension to the approach in Ref. 4 by introducing a different feedback linearization scheme, useful for systems with high relative degree. Incorporating prior knowledge of the nonlinear system dynamics in the feedback linearization stage may greatly simplify the design of the linear compensator discussed earlier. It is particularly useful for applications in which part of the system dynamics, for example, actuator dynamics, are nearly linear with relatively well-known characteristics. Here we address several theoretical aspects that justify the procedure and that point out several practical design implications. Although presented in conjunction with the direct output feedback scheme of Ref. 4, the proposed linearization procedure can be used with any control design technique that relies on model inversion, for example, that of Ref. 5.

Problem Statement

Let the dynamics of a state observable nonlinear single-input/single-output (SISO) system be given in a state-space form by

$$\dot{\boldsymbol{x}} = \boldsymbol{f}(\boldsymbol{x}, u) \tag{1a}$$

$$y = h(\boldsymbol{x}) \tag{1b}$$

where $\boldsymbol{x} \in \boldsymbol{\Omega}_x \subset \Re^n$ is the state space vector of the system with possibly unknown dimension n, $u \in \Omega_u \subset \Re$ is the system input (control), $y \in \Omega_y \in \Re$ is its output (measurement) signal, and $\boldsymbol{f}(\cdot,\cdot)$, $h(\cdot)$ are unknown functions with appropriate input–output spaces.

Assumption 1. The dynamic system of Eqs. (1) satisfies the input–output feedback linearization conditions[6] with relative degree r.

Assumption 1 implies

$$y^{(i)} = \frac{\mathrm{d}h_{i-1}(\boldsymbol{x})}{\mathrm{d}t} = \frac{\partial h_{i-1}(\boldsymbol{x})}{\partial \boldsymbol{x}} \boldsymbol{f}(\boldsymbol{x}, u) \triangleq h_i(\boldsymbol{x}) \tag{2}$$

for $i = 1, \ldots, r-1$ with $h_0(\boldsymbol{x}) = h(\boldsymbol{x})$ and

$$y^{(r)} = \frac{\mathrm{d}h_{r-1}(\boldsymbol{x})}{\mathrm{d}t} \triangleq h_r(\boldsymbol{x}, u) \tag{3}$$

It also implies that the system can be transformed into a normal form[6]

$$\dot{\boldsymbol{y}} = \boldsymbol{h}(\boldsymbol{y}, \boldsymbol{\xi}, u) \tag{4a}$$

$$\dot{\boldsymbol{\xi}} = \boldsymbol{\chi}(\boldsymbol{y}, \boldsymbol{\xi}) \tag{4b}$$

where $y \triangleq [y \;\; \dot{y} \;\; \cdots \;\; y^{(r-1)}]^T$ and $\boldsymbol{\xi} \triangleq [\xi_1 \;\; \xi_2 \;\; \cdots \;\; \xi_{n-r}]^T$.

The output feedback control law discussed in this work is designed so that the system output y tracks a bounded reference signal or trajectory $\boldsymbol{y}_{\mathrm{tr}} \in \Omega_{\mathrm{tr}} \subset \Re$, which is assumed to be r times differentiable with bounded derivatives. The reference trajectory and its derivatives are grouped into $\boldsymbol{y}_{\mathrm{tr}} = [y_{\mathrm{tr}} \;\; \dot{y}_{\mathrm{tr}} \;\; \cdots \;\; y_{\mathrm{tr}}^{(r-1)}]^T$. The tracking error and the tracking error vector are defined as

$$\tilde{y} = y_{\mathrm{tr}} - y \tag{5}$$

$$\tilde{\boldsymbol{y}} = \boldsymbol{y}_{\mathrm{tr}} - \boldsymbol{y} \tag{6}$$

Assumption 2. The system $\dot{\boldsymbol{\xi}} = \boldsymbol{\chi}(\boldsymbol{y}_{\mathrm{tr}}, \boldsymbol{\xi})$ has a unique steady-state solution $\bar{\boldsymbol{\xi}}$. Moreover, with $\tilde{\boldsymbol{\xi}} = \bar{\boldsymbol{\xi}} - \boldsymbol{\xi}$, the system

$$\dot{\tilde{\boldsymbol{\xi}}} = \boldsymbol{\chi}(\bar{\boldsymbol{\xi}}, \boldsymbol{y}_{\mathrm{tr}}) - \boldsymbol{\chi}(\bar{\boldsymbol{\xi}} - \tilde{\boldsymbol{\xi}}, \boldsymbol{y}_{\mathrm{tr}} - \tilde{\boldsymbol{y}}) \triangleq \tilde{\boldsymbol{\chi}}(\tilde{\boldsymbol{\xi}}, \tilde{\boldsymbol{y}}, \bar{\boldsymbol{\xi}}, \boldsymbol{y}_{\mathrm{tr}}) \tag{7}$$

has a continuously differentiable function $V_{\tilde{\xi}}(t, \tilde{\boldsymbol{\xi}})$ that satisfies

$$\eta_1 \|\tilde{\boldsymbol{\xi}}\|^2 \le V_{\tilde{\xi}}(t, \tilde{\boldsymbol{\xi}}) \le \eta_2 \|\tilde{\boldsymbol{\xi}}\|^2 \tag{8a}$$

$$\frac{\mathrm{d}V_{\tilde{\xi}}(t, \tilde{\boldsymbol{\xi}})}{\mathrm{d}t} \le -\eta_3 \|\tilde{\boldsymbol{\xi}}\|^2 + \eta_4 \|\tilde{\boldsymbol{\xi}}\| \|\tilde{\boldsymbol{y}}\| \tag{8b}$$

where $\eta_1, \eta_2, \eta_3 > 0$ and $\eta_4 \ge 0$ are independent of $\boldsymbol{y}_{\mathrm{tr}}$.

This assumption implies that the zero dynamics of the original system in Eqs. (1) are exponentially stable and the system is minimum phase.

Controller Design

The output feedback controller design is based on a nonstandard dynamic model linearization, linear dynamic compensation of the linearized system, and adaptive NN-based compensation of the model linearization error.

Received 7 November 2002; revision received 25 November 2003; accepted for publication 30 December 2003.

*Associate Professor, Faculty of Aerospace Engineering. Associate Fellow AIAA.
†Professor, School of Aerospace Engineering. Fellow AIAA.
‡Associate Professor, Department of Aerospace and Ocean Engineering. Member AIAA.

Approximate Feedback Linearization

In a standard feedback linearization scheme, the right-hand side of Eq. (3) is defined as a pseudocontrol input ν. If the function $h_r(\boldsymbol{x}, u)$ is known exactly, this results in a linearized system with r poles at the origin given by

$$y^{(r)} = \nu \tag{9}$$

Then, a linear compensator is designed to stabilize those r poles. In the output feedback setting, this task is not simple for cases of $r > 2$ and may result in an unstable compensator, an undesirable characteristic from a practical implementation perspective. Moreover, linearization of fast dynamics (fast poles in linear systems) to the origin may require unrealistically large, high-frequency actuation.

To overcome these difficulties for systems with high relative degree and/or fast dynamics, an alternative linearization scheme is proposed, in which the poles of the ideally linearized model are shifted away from the origin. These poles can correspond to the poles of a previously known or a predetermined linearized model, related to the full nonlinear system dynamics. For example, when linearizing an unknown nonlinear system with actuators, the poles associated with the latter can be placed at fairly well-known locations of the actuators dynamics, whereas the rest of the poles are conventionally linearized to the origin.

The proposed linearization scheme relies on Assumption 1 and the resulting definitions in Eqs. (2) and (3). Multiplying Eq. (2) by a constant a_i, Eq. (3) by a_0, and summing the result leads to

$$a_0 y^{(r)} + \sum_{i=1}^{r} a_i y^{(r-i)} = a_0 h_r(\boldsymbol{x}, u) + \sum_{i=1}^{r} a_i h_{r-i}(\boldsymbol{x}) \triangleq g_r(\boldsymbol{x}, u) \tag{10}$$

The coefficients $a_i, i = 0, \ldots, r$, are chosen such that the roots of the polynomial defined by

$$p(s) = \sum_{i=0}^{r} a_i s^{(r-i)} \tag{11}$$

with s being a complex (Laplace) variable, are the r poles of the ideally linearized system.

The modified feedback linearization is performed by introducing a redefined pseudocontrol signal given by

$$\nu = \hat{g}_r(y, u) \tag{12}$$

where $\hat{g}_r(y, u)$ is the best available approximation of $g_r(\boldsymbol{x}, u)$. Then, the system dynamics can be expressed as

$$\sum_{i=0}^{r} a_i y^{(r-i)} = \nu + \Delta'(\boldsymbol{x}, y, u) \tag{13}$$

where $\Delta'(\boldsymbol{x}, y, u) = g_r(\boldsymbol{x}, u) - \hat{g}_r(y, u)$. The controller is designed to define the pseudocontrol signal ν. The actual control input u is obtained by inverting the transformation defined in Eq. (12),

$$u = \hat{g}_r^{-1}(y, \nu) \tag{14}$$

which requires that the model approximation function $\hat{g}_r(\cdot, \cdot)$ is chosen to be invertible with respect to its second argument u.

The model linearization accuracy is quantified by the model inversion error $\Delta'(\boldsymbol{x}, y, u)$, which can be redefined using u of Eq. (14) as

$$\Delta'(\boldsymbol{x}, y, u) = \Delta\left[\boldsymbol{x}, y, \hat{g}_r^{-1}(y, \nu)\right] \triangleq \Delta(\boldsymbol{x}, y, \nu) \tag{15}$$

The only difference between $\Delta'(\cdot, \cdot, \cdot)$ and $\Delta(\cdot, \cdot, \cdot)$ is in their third input argument. If inversion is exact, that is, $\Delta = 0$, Eq. (13) represents an rth-order linear system with ν being its input and $p(s)$ of Eq. (11) being its characteristic polynomial. When inversion is not exact, Δ acts as a disturbance.

Output Feedback Control

Following Ref. 4, the pseudocontrol ν in Eq. (13) is constructed to include three main elements,

$$\nu = \nu_{\text{tr}} + \nu_{\text{dc}} - \nu_{\text{ad}} \tag{16}$$

where ν_{dc} is a linear dynamic compensation term designed to achieve the desired dynamic characteristics of the ideally linearized model, ν_{tr} is introduced to achieve asymptotic tracking of the reference trajectory, and ν_{ad} is an adaptive signal designed to compensate approximately the effect of the model inversion error Δ. This definition of the pseudocontrol signal leads to the control architecture of Fig. 1.

Substituting Eq. (16) into Eq. (13), while using the definition in Eq. (15), leads to

$$\sum_{i=0}^{r} a_i y^{(r-i)} = \nu_{\text{tr}} + \nu_{\text{dc}} + [\Delta(\boldsymbol{x}, y, \nu) - \nu_{\text{ad}}] \tag{17}$$

The linear dynamic compensator design is performed using the model of Eq. (17), where the difference $(\Delta - \nu_{\text{ad}})$ is regarded as a disturbance term. The synthesis starts by constructing the tracking error $\tilde{y}$ dynamics equation. To ensure that this equation is not forced

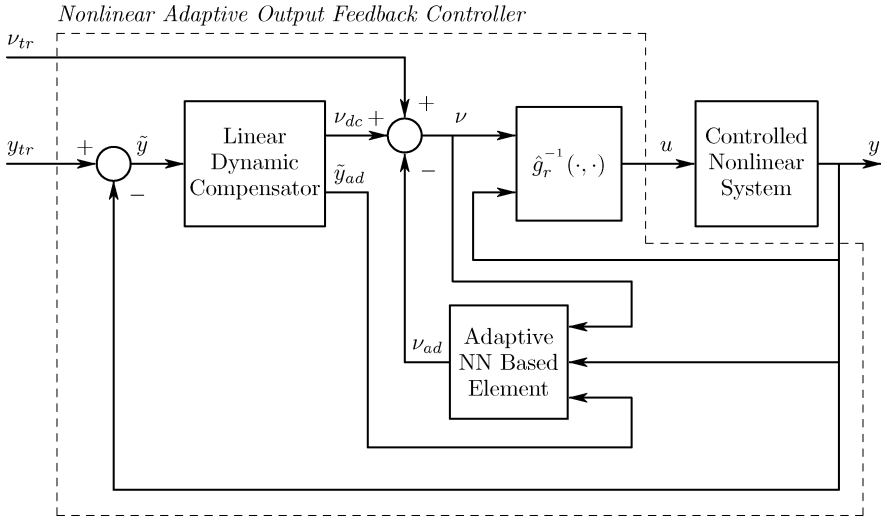

Fig. 1 Control system architecture.

directly by the reference input y_{tr}, the pseudocontrol component ν_{tr} is chosen as

$$\nu_{\text{tr}} = \sum_{i=0}^{r} a_i y_{\text{tr}}^{(r-i)} \tag{18}$$

which implies that y_{tr} should be at least r times differentiable. For that, the reference y_{tr} is generated by forcing an at least rth-order reference model by an external command input. Substituting Eq. (18) into (17), while using Eq. (5) to introduce the tracking error and its time derivatives, results in the open-loop tracking error dynamics equation

$$\sum_{i=0}^{r} a_i \tilde{y}^{(r-i)} = -\nu_{\text{dc}} + (\nu_{\text{ad}} - \Delta) \tag{19}$$

If the right-hand side terms of Eq. (19) are regarded as a control input $-\nu_{\text{dc}}$ and a disturbance $(\nu_{\text{ad}} - \Delta)$, Eq. (19) represents a rth-order linear system of the tracking error dynamics with a transfer function $1/p(s)$.

The linear dynamic compensator is given by

$$\begin{Bmatrix} \nu_{\text{dc}}(s) \\ \tilde{y}_{\text{ad}}(s) \end{Bmatrix} = \frac{1}{D_{\text{dc}}(s)} \begin{bmatrix} N_{\text{dc}}(s) \\ N_{\text{ad}}(s) \end{bmatrix} \tilde{y}(s) \tag{20}$$

where $N_{\text{dc}}/D_{\text{dc}}(s)$ is designed to stabilize $1/p(s)$. For the case where the linearization is defined by Eq. (9), r poles at the origin have to be stabilized, requiring an at least $(r-1)$th-order dynamic compensator.[7] With the modified linearization scheme, $1/p(s)$ may have poles at more favorable locations, which simplifies the linear controller design task and leads to a lower-order compensator.

The effect of the model inversion error is compensated by a Gaussian radial basis function (GRBF) NN given by

$$\Delta(\boldsymbol{\eta}) = \boldsymbol{W}^T \boldsymbol{\phi}(\boldsymbol{\eta}) + \varepsilon(\boldsymbol{\eta}) \tag{21}$$

where $\boldsymbol{\eta} \in \boldsymbol{\Omega}_\eta$ are the variables on which Δ depends, $\boldsymbol{W} \in \Re^N$ is a vector of adjustable NN weights, $\boldsymbol{\phi}(\cdot)$ is a N-dimensional vector of Gaussian basis functions, ε is the NN approximation error, and N is the number of NN neurons. When $\boldsymbol{\eta}$ is confined to a compact set $\boldsymbol{\Omega}_\eta$, a finite weight vector $\boldsymbol{W}^*$ can be found for which

$$|\varepsilon(\boldsymbol{\eta})| \le \varepsilon^*, \qquad \forall \quad \boldsymbol{\eta} \in \boldsymbol{\Omega}_\eta \tag{22}$$

The input $\boldsymbol{\eta}$ to the NN should comprise the variables on which Δ depends, that is, $(\boldsymbol{x}, y, \nu)$. Because $\boldsymbol{x}$ is not available for feedback, based on the recent result of Ref. 8, for an observable system, the measured output y, the pseudocontrol ν, and their stored previous values, combined in $\bar{\boldsymbol{\eta}}$, can be used as the NN inputs to approximate Δ

$$\Delta(\boldsymbol{\eta}) = \boldsymbol{W}^{*T} \boldsymbol{\phi}(\bar{\boldsymbol{\eta}}) + \varepsilon(\bar{\boldsymbol{\eta}}), \qquad |\varepsilon| < \varepsilon^* \tag{23}$$

The actual adaptive signal ν_{ad} is set to

$$\nu_{\text{ad}} = \hat{\boldsymbol{W}}^T \boldsymbol{\phi}(\bar{\boldsymbol{\eta}}) \tag{24}$$

where $\hat{\boldsymbol{W}}$ is an online computed estimate of $\boldsymbol{W}^*$. When Eqs. (23) and (24) are used, $(\nu_{\text{ad}} - \Delta)$ is expressed as

$$\nu_{\text{ad}} - \Delta = \hat{\boldsymbol{W}}^T \boldsymbol{\phi} - \varepsilon \tag{25}$$

where $\tilde{\boldsymbol{W}} = \hat{\boldsymbol{W}} - \boldsymbol{W}^*$ is the NN weight error.

The NN weight adaptation rule is constructed utilizing the second output of the linear compensator $\tilde{y}_{\text{ad}}$. To ensure that $\tilde{y}_{\text{ad}}$ is a function of measured signals only, the closed-loop transfer function between the forcing term $(\nu_{\text{ad}} - \Delta)$ and $\tilde{y}_{\text{ad}}$, obtained by substituting Eqs. (20) and (24) into (19)

$$\tilde{y}_{\text{ad}}(s) = \frac{N_{\text{ad}}(s)}{p(s)D_{\text{dc}}(s) + N_{\text{dc}}(s)} (\tilde{\boldsymbol{W}}^T \boldsymbol{\phi} - \varepsilon)(s) \triangleq G(s)(\tilde{\boldsymbol{W}}^T \boldsymbol{\phi} - \varepsilon)(s) \tag{26}$$

should be strictly positive real (SPR).[4] For the case of relative degree $r = 1$, the SPR condition can be achieved by a proper choice of N_{ad}. If $r > 1$, the SPR property is achieved by introducing a stable low-pass filter $T^{-1}(s)$ into Eq. (26) through the following manipulation:

$$\begin{aligned} \tilde{y}_{\text{ad}}(s) &= G(s)T(s)T^{-1}(s)(\tilde{\boldsymbol{W}}^T \boldsymbol{\phi} - \varepsilon)(s) \\ &= \bar{G}(s)\left(\tilde{\boldsymbol{W}}^T \boldsymbol{\phi}_f + \delta - \varepsilon_f\right)(s) \end{aligned} \tag{27}$$

where $\bar{G}(s) \triangleq G(s)T(s)$ and $\boldsymbol{\phi}_f$ and ε_f are the signals $\boldsymbol{\phi}$ and ε, respectively, filtered through $T^{-1}(s)$. Here, δ is a mismatch term given by

$$\delta(s) = T^{-1}(s)(\tilde{\boldsymbol{W}}^T \boldsymbol{\phi}) - \tilde{\boldsymbol{W}}^T \boldsymbol{\phi}_f \tag{28}$$

It can be bounded as

$$|\delta| \le c\|\tilde{\boldsymbol{W}}\|, \qquad c > 0 \tag{29}$$

where $\|\cdot\|$ denotes the two norm of a vector[2]. Equation (27) can be stated in state-space form as

$$\dot{\boldsymbol{z}} = A_{\text{cl}} \boldsymbol{z} + B_{\text{cl}}\left(\tilde{\boldsymbol{W}}^T \boldsymbol{\phi}_f + \delta - \varepsilon_f\right) \tag{30a}$$

$$\tilde{y}_{\text{ad}} = C_{\text{cl}} \boldsymbol{z} \tag{30b}$$

while the tracking error $\tilde{y}$ can be shown to be linear in $\boldsymbol{z}$

$$\tilde{\boldsymbol{y}} = C_{\tilde{y}} \boldsymbol{z} \tag{31}$$

The fact that $\bar{G}(s)$ is SPR ensures the existence of $Q > 0$ such that the solution P of

$$A_{\text{cl}}^T P + P A_{\text{cl}} = -Q \tag{32}$$

is positive definite and

$$P B_{\text{cl}} = C_{\text{cl}}^T \tag{33}$$

Equation (30a) implies that all of the components of $\boldsymbol{\phi}$ have to be filtered through $T^{-1}(s)$, which, thus, has to be replicated N times. This can be expressed in a consolidated state-space form as

$$\dot{\boldsymbol{z}}_f = A_f \boldsymbol{z}_f + B_f \boldsymbol{\phi} \tag{34a}$$

$$\boldsymbol{\phi}_f = C_f \boldsymbol{z}_f \tag{34b}$$

Stability of the filter ensures the existence of a positive definite matrix $P_f > 0$ that satisfies the Lyapunov equation

$$A_f^T P_f + P_f A_f = -Q_f \tag{35}$$

for any positive definite $Q_f > 0$.

The signals $\tilde{y}_{\text{ad}}$ and $\boldsymbol{\phi}_f$ are used in the following NN weight update rule:

$$\dot{\hat{\boldsymbol{W}}} = -F[\tilde{y}_{\text{ad}} \boldsymbol{\phi}_f + \sigma_W \hat{\boldsymbol{W}}] \tag{36}$$

where $F > 0$ and $\sigma_w > 0$ are the adaptation gains.

The consequent stability analysis is performed in an expanded closed-loop error signal space, comprising $\boldsymbol{\mu} \triangleq [\boldsymbol{z}^T \;\; \boldsymbol{z}_f^T \;\; \tilde{\boldsymbol{W}}^T \;\; \tilde{\boldsymbol{\xi}}^T]^T$, whereas the NN approximation holds over a compact set $\boldsymbol{\Omega}_\eta$ defined in the space of the original variables. Because the pseudocontrol ν is a function of $\boldsymbol{z}$, $\boldsymbol{z}_f$, and $\hat{\boldsymbol{W}}$, and because y can be functionally related to $\boldsymbol{z}$ and y_{tr}, the compact set $\boldsymbol{\Omega}_\eta$ can be (implicitly) mapped into a compact set in the space of $\boldsymbol{\mu}$, which we denote $\boldsymbol{\Omega}_\mu$. The stability analysis will require an assumption regarding the size of $\boldsymbol{\Omega}_\mu$. For that, let $\mathscr{B}_R$ be the largest hypersphere enclosed in $\boldsymbol{\Omega}_\mu$, that is,

$$\mathscr{B}_R = \{\boldsymbol{\mu} \mid \|\boldsymbol{\mu}\| \le R\} \tag{37}$$

where $R = \arg\max_{x>0} (\boldsymbol{\mu} \in \boldsymbol{\Omega}_\mu \text{ and } \|\boldsymbol{\mu}\| \le x)$.

Assumption 3. The compact set Ω_η over which the NN approximation holds is large enough to ensure that

$$R > \rho\sqrt{\frac{\Pi_{2_M}}{\Pi_{1_m}}} \triangleq \frac{\beta\sqrt{\Pi_{2_M}/\Pi_{1_m}}}{\min(\alpha_z, \alpha_{z_f}, \alpha_w, \alpha_\xi)} \tag{38}$$

where the positive constants α_z, α_{z_f}, α_W, α_ξ, and β are defined by

$$\alpha_z^2 = \tfrac{1}{2}\left[Q_m - (\varepsilon^* + c)\|PB_{\rm cl}\| - \eta_4^2\bar{\sigma}_C^2/\eta_3\right] > 0 \tag{39a}$$

$$\alpha_{z_f}^2 = \tfrac{1}{2}[Q_{fm} - \bar{\phi}\|P_f B_f\|] > 0 \tag{39b}$$

$$\alpha_W^2 = [\sigma_W - 1 - c\|PB_{\rm cl}\|/2] > 0 \tag{39c}$$

$$\alpha_\xi^2 = \eta_3/2 \tag{39d}$$

$$\beta^2 = \tfrac{1}{2}\left[\varepsilon^*\|PB_{\rm cl}\| + \bar{\phi}\|P_f B_f\| + \sigma_W^2\bar{W}^2/2\right] \tag{39e}$$

Q_m and Q_{fm} are the minimum eigenvalues of Q and Q_f, $P > 0$ and $P_f > 0$ are, respectively, solutions of Eqs. (32) and (35) for $Q > 0$ and $Q_f > 0$ satisfying the conditions in Eqs. (39a) and (39b), $\bar{\sigma}_C$ is the maximum singular value of $C_{\tilde{y}}$ in Eq. (31), $\|\phi(\bar{\eta})\| \le \bar{\phi}$ by the definition of GRBFs, $\tilde{W}$ is a bound on the NN weights $\|W^*\| \le \tilde{W}$, Π_{1_m} is the minimum eigenvalue of the matrix Π_1, and Π_{2_M} is the maximum eigenvalue of the matrix Π_2, defined by

$$\Pi_1 = \tfrac{1}{2}\,\text{blockdiag}\left(P, P_f, F^{-1}, 2\eta_1 I_{(n-r)\times(n-r)}\right) \tag{40a}$$

$$\Pi_2 = \tfrac{1}{2}\,\text{blockdiag}\left(P, P_f, F^{-1}, 2\eta_2 I_{(n-r)\times(n-r)}\right) \tag{40b}$$

Finally, the adaptation gain σ_W is chosen so that

$$\sigma_W > 1 + c\|PB_{\rm cl}\|/2 \tag{41}$$

Uniform Ultimate Boundedness

The uniform ultimate boundedness of the tracking error will be shown using the following positive definite Lyapunov function candidate:

$$V = \tfrac{1}{2}z^T Pz + \tfrac{1}{2}z_f^T P_f z_f + \tfrac{1}{2}\tilde{W}^T F^{-1}\tilde{W} + V_{\tilde{\xi}} \tag{42}$$

where $V_{\tilde{\xi}}$ satisfies the conditions in Eqs. (8). In addition, the theorem statement relies on the largest level set of V inside Ω_μ, which we denote by $\Omega_{V_{\max}}$.

Theorem. Let $y_{\rm tr}$ be a bounded reference trajectory with continuous and bounded derivatives $y_{\rm tr}^{(i)}$, $i = 1, \ldots, r$, where r is the relative degree of the system defined by Eqs. (1). The output y is required to track $y_{\rm tr}$. Consider the output feedback controller defined by Eqs. (10), (12), (14), (16), (18), (20), and (24) and the adaptation rule given by Eqs. (34) and (36). Then, the closed-loop error signal μ is uniformly ultimately bounded provided that Assumptions 1–3 hold and that the initial error signal complies with $\mu(0) \in \Omega_{V_{\max}}$.

Proof. Consider the positive definite Lyapunov function candidate of Eq. (42). The time derivative of V, while using the dynamics of Eqs. (30a) and (34a), is

$$\dot{V} = -\tfrac{1}{2}z^T Qz + z^T PB_{\rm cl}\left(\tilde{W}^T\phi_f + \delta - \varepsilon_f\right) - \tfrac{1}{2}z_f^T Q_f z_f + z_f^T P_f B_f\phi + \tilde{W}^T F^{-1}\dot{\tilde{W}} + \dot{V}_{\tilde{\xi}} \tag{43}$$

Incorporating the SPR result of Eq. (33) and the adaptation rule of Eq. (36) leads to

$$\dot{V} = -\tfrac{1}{2}z^T Qz + z^T PB_{\rm cl}(\delta - \varepsilon_f) - \tfrac{1}{2}z_f^T Q_f z_f + z_f^T P_f B_f\phi - \sigma_W\tilde{W}^T(\tilde{W} + W^*) + \dot{V}_{\tilde{\xi}} \tag{44}$$

Assuming that the filter $T^{-1}(s)$ is scaled so that its maximum gain is unity, and using the NN accuracy bound of Eq. (23), the filtered error ε_f can be bounded as $|\varepsilon_f| \le |\varepsilon| \le \varepsilon^*$. When this bound is used together with the bounds on the mismatch term δ given by Eq. (29) and $\dot{V}_{\tilde{\xi}}$ of Eqs. (8b), the derivative in Eq. (44) can be bounded as

$$\dot{V} \le -\tfrac{1}{2}Q_m\|z\|^2 + c\|PB_{\rm cl}\|\|z\|\|\tilde{W}\| + \varepsilon^*\|PB_{\rm cl}\|\|z\| - \tfrac{1}{2}Q_{fm}\|z_f\|^2 + \bar{\phi}\|P_f B_f\|\|z_f\| - \sigma_W\|\tilde{W}\|^2 + \sigma_W\bar{W}\|\tilde{W}\| - \eta_3\|\tilde{\xi}\|^2 + \eta_4\|\tilde{\xi}\|\|\tilde{y}\| \tag{45}$$

When squares are completed and the definitions of Eqs. (39) are used, $\dot{V}$ can be further overbounded, as

$$\dot{V} \le -\alpha_z^2\|z\|^2 - \alpha_{z_f}^2\|z_f\|^2 - \alpha_W^2\|\tilde{W}\|^2 - \alpha_\xi^2\|\tilde{\xi}\|^2 + \beta^2 \tag{46}$$

Setting the right-hand side of Eq. (46) to zero defines an edge of a compact set in the closed-loop error signal μ space. This compact set, denoted by $\Omega_{\dot{V}}$, is a hyperellipsoid centered at the origin of the μ space, outside of which $\dot{V} < 0$. Assumption 3 guarantees that $\Omega_{\dot{V}}$ is inside the compact set over which the NN approximation holds. □

The following remarks provide design guidelines, which can be utilized to ensure that the conditions in Assumption 3 are met.

1) From Eq. (38), it is clear that it is advantageous to choose the design parameters such that β is small while α_z, α_{z_f}, α_w, and α_ξ are large. In addition, $\kappa_\Pi = \Pi_{2_M}/\Pi_{1_m}$ should be kept as small as possible.

2) Choosing large eigenvalues for $A_{\rm cl}$, that is, fast closed-loop poles of the linearized system, implies large eigenvalues for the Lyapunov operator $A_{\rm cl}^T P + PA_{\rm cl}$ and hence a small solution P of Eq. (32) for a given Q. This will lead to a large difference between Q_m and $\|PB_{\rm cl}\|$ and, according to Eq. (39a), potentially a large α_z. The same logic applies to the choice of A_f to make α_{z_f} large.

3) Equation (39c) motivates the choice of a large adaptation gain σ_w. However, the dependance of β on σ_w, given by Eq. (39e), and the requirement to keep β small, introduces an upper bound on the adaptation gain σ_w.

4) The requirement for a small κ_Π is more complex to control due to the unknown parameters η_1 and η_2 and their relative magnitude. Nevertheless, some design guidelines can be drawn by noting that

$$\kappa_\Pi = \frac{\max\{\Pi_M, \eta_2\}}{\min\{\Pi_m, \eta_1\}} \tag{47}$$

where Π_M and Π_m are the maximum and minimum eigenvalues of $\Pi = \text{blockdiag}\,(P, P_f, F^{-1})$, which does not depend on the unknowns η_1 and η_2. Equation (47) implies that it is advantageous to make $\Pi_M \approx \Pi_m$, or equivalently, to choose the matrices P, P_F, and F so that all of their eigenvalues are approximately equal among each other. This means that if one of these matrices is changed, the same change should be applied to the other two to keep $\Pi_M \approx \Pi_m$.

5) For fixed values of R and ρ, the inequality in Eq. (38) implies upper and lower limits for the adaptation gain matrix F. If $F = \gamma I$ with a large γ, the minimum eigenvalue of Π_{1_m} is determined by the value of γ and Eq. (38) implies an upper bound $\gamma < (R/\rho)^2/\Pi_{2_M}$ on the adaptation gain. Likewise, for small γ, so that the maximum eigenvalue of Π_{2_M} is determined by the value of γ, we have $\gamma > (\rho/R)^2/\Pi_{1_m}$ as a lower bound.

Fuel Slosh Example

In this example, we examine the dynamic interaction between a spacecraft attitude control system and propellant sloshing in partially filled tanks. If the frequency of the first sloshing mode, which changes with the fuel mass variations, is less than about six times the attitude control bandwidth, this interaction may lead to instability.[9] As an alternative to a gain-scheduled control design, an adaptive fixed-gain control solution is presented that utilizes the methodology discussed in this Note.

In the current study, we adopt a simulation model of a spacecraft with a spherical partially filled fuel tank, including only the

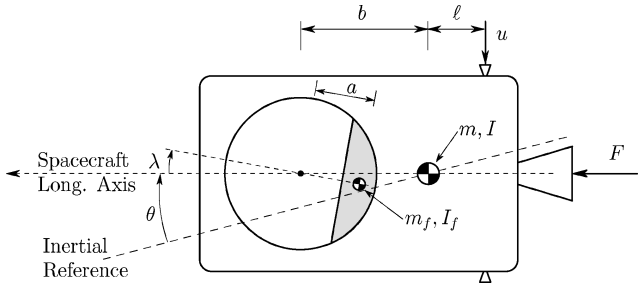

Fig. 2 Model of a spacecraft with a spherical fuel tank during a thrust maneuver.

lowest frequency sloshing mode.[9] This mode is well approximated by considering the fuel to be frozen into a lump that slides with a small friction force acting on the sides of the tank. The result is a pendulumlike motion with its support point at the center of the tank. Only longitudinal motion in the orbital plane is considered. Attitude control is achieved using reaction jets, as is shown in Fig. 2. Figure 2 also presents the geometry and inertial properties of the spacecraft and fuel tank system. There, m and m_f are the masses of the spacecraft and the fuel lump, respectively, and I and I_f are the spacecraft and fuel lump moments of inertia about their respective centers of mass. F is the maneuver thrust, whereas u is the thrust of the reaction jets used for attitude control.

The equations of motion for the rotational degrees of freedom of the system are given by[9]

$$I^*\dot{\omega} - I_c^*\dot{\omega}_f = (\ell + b^*)u - m^*ab\omega_f^2 \sin\lambda + C\dot{\lambda} \tag{48a}$$

$$-I_c^*\dot{\omega} + I_f^*\dot{\omega}_f = -a^*u\cos\lambda - a^*F\sin\lambda + m^*ab\omega^2\sin\lambda - C\dot{\lambda} \tag{48b}$$

$$\dot{\lambda} = \omega_f - \omega \tag{48c}$$

$$\dot{\theta} = \omega \tag{48d}$$

$$\dot{u} = (1/\tau_r)(u_c - u) \tag{48e}$$

where

$$I^* \triangleq I + m^*b^2, \qquad m^* \triangleq mm_f/(m + m_f)$$

$$I_f^* \triangleq I_f + m^*a^2, \qquad a^* \triangleq am_f/(m + m_f)$$

$$I_c^* \triangleq m^*ab\cos\lambda, \qquad b^* \triangleq bm_f/(m + m_f) \tag{49}$$

and C is the slosh damping coefficient. The reaction jet is modeled as a first-order system in Eq. (48e) with a time constant τ_r. The measured and controlled variable is the spacecraft pitch attitude θ that has a relative degree three with respect to the reaction jet command input u_c. For small angles and angular rates, the transfer function between θ and u_c is given by

$$\frac{\theta}{u_c}(s) = K\frac{1}{s^2}\frac{s^2 + 2\zeta_z\omega_z s + \omega_z^2}{s^2 + 2\zeta_p\omega_p s + \omega_p^2}\frac{1}{1 + \tau_r s} \tag{50}$$

where

$$K = \frac{(\ell + b^*)I_f^* - a^*I_c^*}{I^*I_f^* - \left(I_c^*\right)^2}$$

$$\omega_z^2 = \frac{a^*F}{I_f^* - a^*I_c^*/(\ell + b^*)}, \qquad \zeta_z = \frac{C(\ell + b^* - a^*)}{2\omega_z}$$

$$\omega_p^2 = \frac{a^*F\left(I^* - I_c^*\right)}{I^*I_f^* - \left(I_c^*\right)^2}, \qquad \zeta_p = \frac{C\left[I + I_f + (b - a)^2\right]}{2\omega_p} \tag{51}$$

When $I^* > I_c^*$, $I^*I_f^* > (I_c^*)^2$, $(\ell + b^*) > a^*$, and $(\ell + b^*)I_f^* > a^*I_c^*$, which is often the case in actual spacecraft, Eqs. (50) and (51) show that the spacecraft/fuel system is minimum phase in the neighborhood of the equilibrium point at the origin.

To simplify the linear compensator design, based on Eq. (50), the relative degree three system dynamics are approximately linearized as

$$(\theta/u_c)(s) = \hat{K}(1/s^2)[1/(1 + \hat{\tau}_r s)] \triangleq \hat{K}/p(s) \tag{52}$$

or alternatively

$$\hat{\tau}_r\,\dddot{\theta} + \ddot{\theta} = \hat{K}u_c \triangleq \nu \tag{53}$$

that is, two poles of the linearized system are kept at the origin, whereas the actuator pole is chosen at its estimated location $-1/\hat{\tau}_r$. The estimated system gain $\hat{K}$ is used to compute the actual reaction jet command by

$$u_c = \nu/\hat{K} \tag{54}$$

The typical physical system parameters used in the simulation are $m = 600$ kg, $I = 720$ kg·m^2, $m_f = 300$ kg, $I_f = 150$ kg·m^2, $a = 0.32$ m, $b = 0.25$ m, $\ell = 0.2$ m, $C = 1$ kg·m^2/s, $F = 500$ N, and $\tau_r = 0.1$ s. For this case, the parameters of the transfer function in Eq. (50) are $K = 3.74 \times 10^{-4}$ (kg·m)$^{-1}$, $(\omega_z, \zeta_z) = (0.57, 3.3 \times 10^{-3})$, and $(\omega_p, \zeta_p) = (0.55, 6.3 \times 10^{-4})$, where (ω_z, ω_p) are given in radians per second. Because $\omega_z > \omega_p$, this introduces a destabilizing fuel sloshing mode.[9] The control design model of Eq. (53) assumes a 50% overestimated control effectiveness, that is, $\hat{K} = 1.5K \approx 5.6 \times 10^{-4}$ (kg·m)$^{-1}$ and $\hat{\tau}_r = \tau_r$.

A lead compensator was designed so that the dominant closed-loop poles have a natural frequency of $\omega_{\text{cl}} = 1$ rad/s and damping coefficient $\zeta = 0.8$. Choosing $N_{\text{ad}}(s)$ and $T(s)$ to meet the SPR condition of Eq. (27), the one-input/two-output lead compensator is given by

$$\begin{Bmatrix} \nu_{\text{dc}}(s) \\ \tilde{y}_{\text{ad}}(s) \end{Bmatrix} = \frac{1}{s + 2.82}\begin{bmatrix} 2.60(s + 0.36) \\ 6(s + 1) \end{bmatrix}\tilde{y}(s) \tag{55}$$

and the SPR low-pass filter $T^{-1}(s)$ is

$$T^{-1}(s) = 1/(s/3 + 1)(s/4 + 1) \tag{56}$$

A third-order linear reference model was used to command the spacecraft attitude. Two complex poles of the reference model have a natural frequency of 0.5 rad/s and damping of 0.8, whereas the real pole has a time constant of 1 s. According to the definition of $p(s)$ in Eq. (52), the pseudocontrol component ν_{tr} associated with the attitude command was set to

$$\nu_{\text{tr}} = 0.1\,\dddot{\theta}_{\text{tr}} + \ddot{\theta}_{\text{tr}} \tag{57}$$

The NN was constructed using five GRBF neurons and a bias. The inputs to the NN were the current and the three delayed values of measured attitude θ and the current and the two delayed values of the pseudocontrol ν. The delay time was set to $\tau = 0.05$ s. The NN adaptation gains were $F = 100$ and $\sigma_w = 2$.

The performance of the adaptive controller was evaluated in a thrust maneuver, which was initialized with the spacecraft attitude aligned with the reference and with fuel center of gravity offset by 10 deg, that is, $\theta(0) = 0$ rad and $\lambda(0) = \pi/18$ rad. An attitude change command of 20 deg is issued at 10 s. The response of the spacecraft controlled with only the linear dynamic compensator is examined first. It exhibits a fuel slosh angle oscillation at an increasing amplitude, reaching 180 deg at about 140 s. Then it starts rotating in the tank at about 0.1 Hz, which induces a limit cycle of about 2.5-deg amplitude in the attitude response.

The same maneuver is repeated next with the adaptive output feedback controller. The attitude and fuel slosh angles for this case are shown in Fig. 3 and demonstrate accurate attitude tracking and

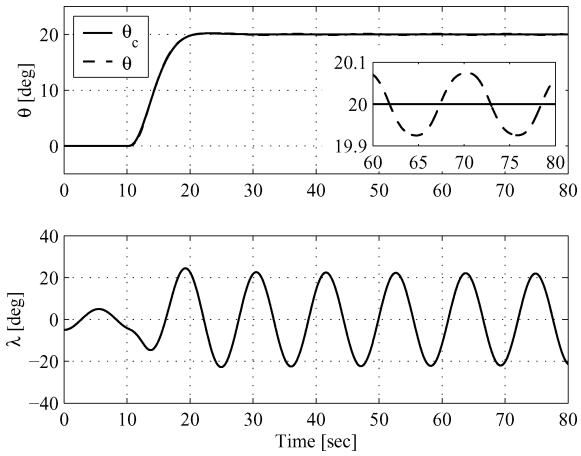

Fig. 3 Response with adaptive output feedback controller: a) spacecraft attitude θ and b) fuel slosh angle λ.

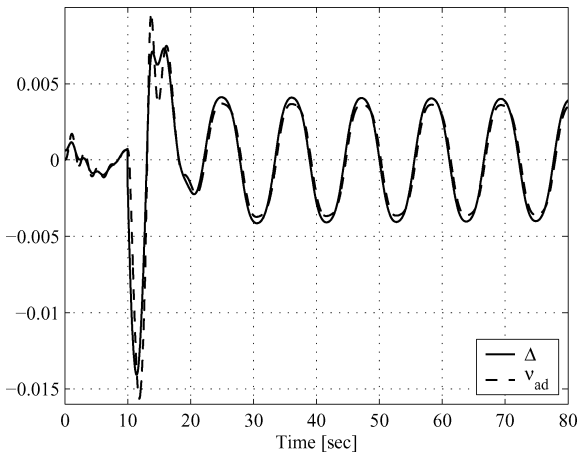

Fig. 4 Computed model inversion error Δ and its NN estimate ν_{ad}.

slowly decaying fuel sloshing. This slow decay is attributed to the fact that the only mechanism for absorbing the fuel motion, while the spacecraft attitude is almost constant, is the small friction force. The adaptive controller eliminates the excitation of the sloshing mode and dramatically reduces its effect on the attitude response. This is illustrated in the insert at the top of Fig. 3, which shows a small decaying oscillation with an amplitude of about 0.075 deg at 80 s. The performance of the adaptive element is shown in Fig. 4, which shows a close match between the computed model inversion error Δ and the adaptive signal ν_{ad}.

Conclusions

This Note presents a nonstandard feedback linearization scheme that can enhance model-inversion-based control design paradigms. This scheme is examined in conjunction with a recently published direct output feedback design approach for nonlinear SISO systems with known relative degree. The controller synthesis comprises the proposed feedback linearization scheme coupled with a linear compensator design and an adaptive NN-based element used to reduce the effect of model inversion errors. Prior knowledge or partial information about the open-loop system dynamics can be incorporated in the design through the proposed linearization procedure. Consequently, the design of the linear compensator can be simplified, usually leading to lower-order compensators. This feature is particularly important for systems with relative degree greater than two, where the linear design step can be challenging. The stability proof provides important design and parameter tuning guidelines, which are instrumental in ensuring uniform ultimate boundedness of the closed-loop system errors.

Acknowledgments

This research was partly sponsored by the fund for the promotion of research at the Technion and by U.S. Air Force Office of Scientific Research Contracts F49620-01-1-0024 and F49620-03-1-0443.

References

[1]Chen, F. C., and Khalil, H. K., "Adaptive Control of Nonlinear Systems using Neural Networks," *International Journal of Control*, Vol. 55, No. 6, 1992, pp. 1299–1317.

[2]Kim, Y., and Lewis, F. L., *High Level Feedback Control with Neural Networks*, World Scientific, River Edge, NJ, 1998.

[3]Rysdyk, R., and Calise, A. J., "Nonlinear Adaptive Flight Control Using Neural Networks," *IEEE Controls Systems Magazine*, Vol. 18, No. 6, 1998, pp. 14–25.

[4]Calise, A. J., Hovakimyan, N., and Idan, M., "Adaptive Output Feedback Control of Nonlinear Systems Using Neural Networks," *Automatica*, Vol. 37, No. 8, 2001, pp. 1201–1211.

[5]Hovakimyan, N., Nardi, F., Calise, A. J., and Kim, N., "Adaptive Output Feedback Control of Uncertain Systems Using Single Hidden Layer Neural Networks," *IEEE Transactions on Neural Networks*, Vol. 13, No. 6, 2002, pp. 1420–1431.

[6]Isidori, A., *Nonlinear Control Systems*, Springer-Verlag, Berlin, 1995.

[7]Brasch, J., and Pearson, J., "Pole Placement using Dynamic Compensators," *IEEE Transactions on Automatic Control*, Vol. 15, No. 1, 1970, pp. 34–43.

[8]Lavretsky, E., Hovakimyan, N., and Calise, A. J., "Upper Bounds for Approximation of Continuous-Time Dynamics Using Delayed Outputs and Feedforward Neural Networks," *IEEE Transactions on Automatic Control*, Vol. 48, No. 9, 2003, pp. 1606–1610.

[9]Bryson, A. E. J., *Control of Spacecraft and Aircraft*, Princeton Univ., Press, Princeton, NJ, 1994, pp. 129–131.

Guidance of Unmanned Air Vehicles Based on Fuzzy Sets and Fixed Waypoints

Mario Innocenti,* Lorenzo Pollini,† and Demetrio Turra‡
University of Pisa, 56126 Pisa, Italy

I. Introduction

THE problem of guidance and control of unmanned aerial vehicles (UAVs) has become a topic of research in recent years. Typical projected UAV operations such as surveillance, payload delivery, and search and rescue can be addressed by waypoint-based guidance. Automatic target recognition, for instance, requires that the aircraft approach the possible target from one or more desired directions. In a highly dynamic cooperative UAV environment, the management system, either centralized or decentralized, may switch the waypoint set rapidly to change an aircraft mission depending on external events, pop-up threats, etc.; the new waypoint set may be ill-formed in terms of flyability (maximum turn rates, descent speed, acceleration, etc.). Although fuzzy logic methods have been applied in the past—see for instance Ref. 1, where Mamdami rules were

Presented as Paper 2002-4993 at the Guidance, Navigation and Control, Monterey, CA, 8 August 2002; received 26 May 2003; revision received 30 October 2003; accepted for publication 11 November 2003.

*Full Professor, Department of Electrical Systems and Automation. Associate Fellow AIAA.

†Postdoctoral Fellow, Department of Electrical Systems and Automation.

‡Ph.D. Student, Department of Electrical Systems and Automation.